EVS30 Symposium
Stuttgart, Germany, October 9 - 11, 2017

Modelling of the power converter with multi-operating mode

Wang Feng, Luo Yutao*
School of Mechanical and Automotive Engineering, South China University of Technology, Guangzhou, PRC, 510641l,
**Corresponding author, ctytluo@scut.edu.cn*

Summery
In this paper, a power converter with multi-operating mode (PCMM) is presented, and its dynamic model is derived. There are three operation modes of the converter, bidirectional DC/DC, AC/DC, and DC/AC. The bidirectional DC/DC mode can be used for bidirectional conversion between two kinds of DC power sources in electric vehicles. The AC/DC mode can convert the single-phase AC source to the DC source, which can charge the battery pack. The DC/AC mode converts the DC power into single-phase AC power and supplies power to the electrical equipment, or supplies energy back to the grid. In this paper, the dynamic model of each mode is derived, and the control method is given. In order to verify the PCMM converter, a simulation model and an experimental prototype is built for testing.

Keywords: Power converter, bidirectional DC/DC, AC/DC, DC/AC

1 Introduction

There are multiple energy sources in electric vehicles. In order to perform energy conversion between different energy sources, a power converter with different functions is needed to meet the voltage matching between the energy sources. For example, in a multi energy storage system consisting of a fuel cell, a supercapacitor, or a battery pack, the voltage levels of each energy source are different, and a DC voltage matching between different energy sources is required[1-4]. In order to recharge the battery, a switch between AC and DC power sources is needed to convert AC power to DC power[5, 6]. Many power equipment requires single-phase alternating current, such as computers, induction cooker, television, etc. In outdoor activities, the DC power of a battery pack is converted into alternating current in order to meet the needs of these electrical equipment. In order to carry out these transformations, at least three converters are needed, which are larger in size and higher in cost.

To enable converters to have multiple functions, researchers have done a lot of work. Literature[7] introduces a structure which integrates the AC/DC converter and the motor controller, which can realize the functions of single phase AC to DC, and DC to three-phase AC. Literature [8, 9] integrates the AC/DC battery charger with the boost DC/DC to achieve the functions of single-phase AC to DC and boost DC/DC.

This paper presents a PCMM converter and builds the dynamic model of the system. The PCMM converter has three working modes, bidirectional DC/DC, AC/DC, and DC/AC mode, respectively. In this paper, the system model in deferent modes are present, the control method are designed, and the simulation and experiment are carried out.

2 Modelling of the system

The PCMM proposed in this paper has three modes. The topology is shown in Fig.1. When working in Bi-DC/DC mode, the switch K_2 is turned on and the switch K_1 is turned off. The system can work in Buck mode

or Boost mode. In AC/DC mode, the switch K_1 is turned on and the switch K_2 is turned off, the system constituted bridgeless PFC topology, the energy flows from the grid to the battery side. In DC/AC inverter model, the switch K_1 is turned on and the switch K_2 is turned off. The energy flow from the battery side to the AC side to achieve DC to AC conversion.

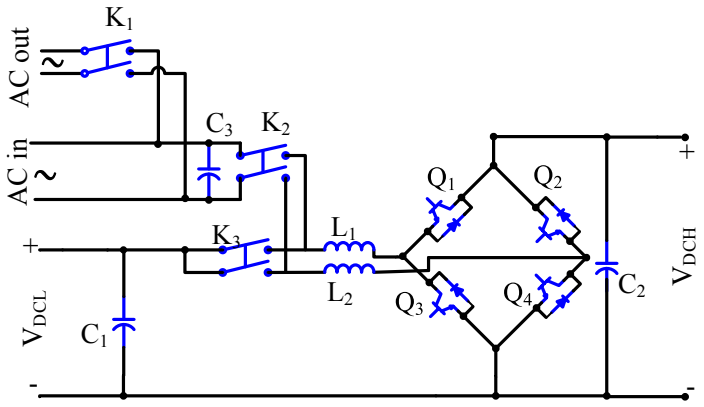

Fig. 1 Proposed topology

2.1 Bi-DC/DC mode

In the Buck mode of the Bi-DC/DC, the equivalent circuit of the system is show in Fig. 2.

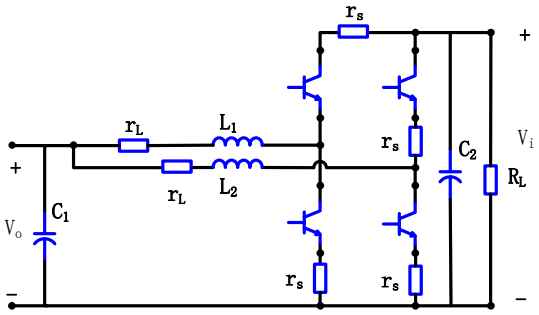

Fig. 2 The equivalent circuit of the Bi-DC/DC mode

Set terminal voltage $v_c(t)$ of the capacitor C_2, inductor current $i_{L1}(t)$, $i_{L2}(t)$ as the state variable of the system, the high side voltage $v_i(t)$ as the input variable, the low side voltage $v_o(t)$ as the output variable. The state space equation of the system and the output equation are Eq.(1), Eq.(2).

$$\begin{bmatrix} \dot{i}_{L1}(t) & \dot{i}_{L2}(t) & \dot{v}_c(t) \end{bmatrix} = A\begin{bmatrix} i_{L1}(t) & i_{L2}(t) & v_c(t) \end{bmatrix}^T + B\begin{bmatrix} v_i(t) \end{bmatrix} \tag{1}$$

$$v_o(t) = C\begin{bmatrix} i_{L1}(t) & i_{L2}(t) & v_c(t) \end{bmatrix}^T + D\begin{bmatrix} v_i(t) \end{bmatrix} \tag{2}$$

For bidirectional DC/DC operating in an inductor continuous mode (CCM), the coefficient matrix of the state space averaged equation is Eq.(3).

$$A = \begin{bmatrix} -\frac{r_s + r_L}{L_1} & 0 & -\frac{1}{L_1} \\ 0 & -\frac{r_s + r_L}{L_2} & -\frac{1}{L_2} \\ \frac{1}{C_1} & \frac{1}{C_1} & -\frac{1}{R_L C_1} \end{bmatrix}, \quad B = \begin{bmatrix} \frac{d}{L_1} \\ \frac{d}{L_2} \\ 0 \end{bmatrix}, \quad C = \begin{bmatrix} 0 & 0 & 1 \end{bmatrix}, \quad D = \begin{bmatrix} 0 \end{bmatrix} \tag{3}$$

Where, the r_L is the internal resistance of inductor L_1 and L_2, r_s is the internal resistance of the IGBT, d is the duty cycle of the PWM.

In steady state, the derivative of each state variable is 0, and the relation between the steady state output voltage and the input voltage can be expressed as Eq.(4).

$$V_o = \frac{2R_L d}{2R_L + r_L + r_s} V_i \tag{4}$$

Where, R_L is the load resistance.

The average vector of the system can be expressed as the sum of the steady-state quantity and the small signal quantity, showing in Eq.(5).

$$\begin{bmatrix} \langle i_{L1}(t) \rangle_{T_s} & \langle i_{L2}(t) \rangle_{T_s} & \langle v_c(t) \rangle_{T_s} \end{bmatrix}^T = \begin{bmatrix} I_{L1} & I_{L2} & V_c \end{bmatrix}^T + \begin{bmatrix} \hat{i}_{L1}(t) & \hat{i}_{L2}(t) & \hat{v}_c(t) \end{bmatrix}^T \tag{5}$$

In the vicinity of the steady state, the small signal model of the system can be obtained by the partial derivative of the variable, and the Laplace transform can be used as Eq.(6).

$$s\begin{bmatrix} \hat{i}_{L1}(s) & \hat{i}_{L2}(s) & \hat{v}_c(s) \end{bmatrix}^T = A\begin{bmatrix} \hat{i}_{L1}(s) & \hat{i}_{L2}(s) & \hat{v}_c(s) \end{bmatrix}^T + B\hat{v}_i(s) + \begin{bmatrix} \frac{V_i}{L_1} & \frac{V_i}{L_2} & 0 \end{bmatrix}^T \hat{d}(s) \tag{6}$$

Make $\hat{d}(s) = 0$， the transfer function of the input voltage to each state variable can be determined as Eq.(7).

$$G_{xvi} = \left(SI - A\right)^{-1} B \tag{7}$$

Make $\hat{v}_i(s) = 0$， the transfer function of the duty cycle to each state variable can be calculated as Eq.(8).

$$G_{xd} = \left(SI - A\right)^{-1} \begin{bmatrix} \frac{V_i}{L_1} & \frac{V_i}{L_2} & 0 \end{bmatrix}^T \tag{8}$$

The Boost model and the Buck model have the dual symmetry, and the coefficient matrix of the average state space equation in the Boost mode is Eq.(9).

$$A = \begin{bmatrix} -\frac{r_s + r_L}{L_1} & 0 & -\frac{1-d}{L_1} \\ 0 & -\frac{r_s + r_L}{L_2} & -\frac{1-d}{L_2} \\ \frac{1-d}{C_2} & \frac{1-d}{C_2} & -\frac{1}{R_L C_2} \end{bmatrix}, \quad B = \begin{bmatrix} \frac{1}{L_1} \\ \frac{1}{L_2} \\ 0 \end{bmatrix}, \quad C = \begin{bmatrix} 0 & 0 & 1 \end{bmatrix}, \quad D = \begin{bmatrix} 0 \end{bmatrix} \tag{9}$$

The relation between the steady state output voltage and the input voltage can be expressed as Eq.(10).

$$V_o = \frac{2R_L(1-d)}{(1-d)^2 2R_L + r_L + r_s} V_i \tag{10}$$

The transfer function of the input voltage to each state variable can be determined as Eq.(11).

$$G_{xvi} = \left(SI - A\right)^{-1} B \tag{11}$$

The transfer function of the duty cycle to each state variable can be calculated as Eq.(12).

$$G_{xd} = \left(SI - A\right)^{-1} \begin{bmatrix} \frac{V_c}{L_1} & \frac{V_c}{L_2} & -\frac{I_{L1}}{C_2} - \frac{I_{L2}}{C_2} \end{bmatrix}^T \tag{12}$$

The control structure of the Bi-DC/DC mode is shown in Fig. 3.

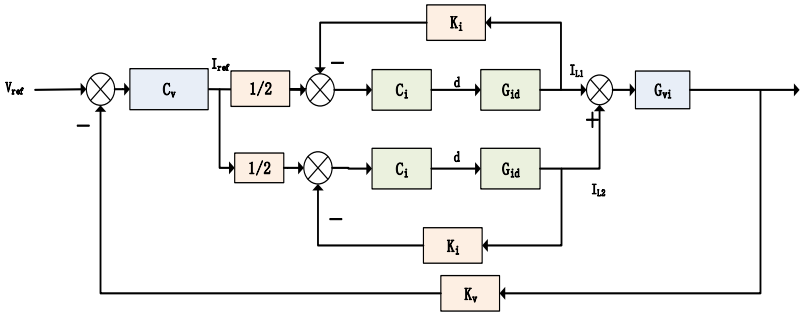

Fig. 3 The control structure of the Bi-DC/DC mode

The system consists of two inner loops and one outer loop of voltage. V_{ref} is the reference voltage, C_v is the voltage loop controller, C_i is the controller for the current loop, K_i is the current gain, K_v is the voltage gain. G_{id} is the transfer function of duty cycle to current, and G_{io} is the transfer function of input voltage to output voltage.

2.2 AC/DC mode

The equivalent circuit of the AC/DC mode is show in Fig. 4.

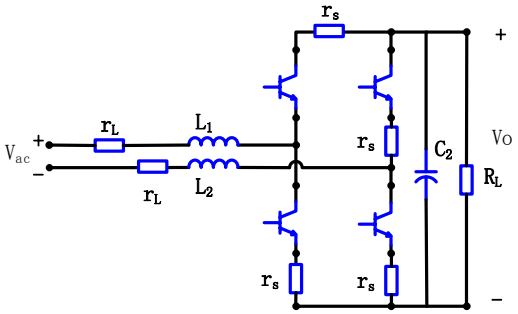

Fig. 4 The equivalent circuit of the AC/DC mode.

As can be seen from the Fig. 4, if the parameters of the four power switches are consistent, the equivalent circuit of the positive half cycle and the negative half cycle is consistent, and only the positive half cycle is modelled and analysed. Set terminal voltage $v_c(t)$ of the capacitor C_2, inductor current $i_{L1}(t)$、$i_{L2}(t)$, as the state variable of the system, the AC side voltage $v_{ac}(t)$ as the input variable, the high side voltage $v_o(t)$ as the output variable. The state space equation of the system and the output equation are Eq.(1), Eq.(2).

Suppose that the internal resistance of four IGBT is equal to r_s, and the internal resistance of the two inductors is equal to r_L, the coefficient matrix of the average state space average equation of the system is Eq.(13).

$$A=\begin{bmatrix} -\dfrac{2r_s+2r_L}{L_1+L_2} & 0 & -\dfrac{1-d}{L_1+L_2} \\ 0 & -\dfrac{2r_s+2r_L}{L_1+L_2} & -\dfrac{1-d}{L_1+L_2} \\ \dfrac{1-d}{C_2} & 0 & -\dfrac{1}{R_LC_2} \end{bmatrix},\quad B=\begin{bmatrix} \dfrac{1}{L_1+L_2} \\ \dfrac{1}{L_1+L_2} \\ 0 \end{bmatrix},\quad C=\begin{bmatrix}0 & 0 & 1\end{bmatrix},\quad D=\begin{bmatrix}0\end{bmatrix} \tag{13}$$

In steady state, the relation between the steady state output voltage and the input voltage can be expressed as Eq.(14).

$$V_o=\frac{R_L(1-d)}{(1-d)^2R_L+2r_L+2r_s}V_i \tag{14}$$

The average vector of the system can be expressed as the sum of the steady-state quantity and the small signal quantity, showing in Eq.(15).

$$\left[\left\langle i_{L1}(t)\right\rangle_{T_s} \quad \left\langle i_{L2}(t)\right\rangle_{T_s} \quad \left\langle v_c(t)\right\rangle_{T_s}\right]^T = \left[I_{L1} \quad I_{L2} \quad V_c\right]^T + \left[\hat{i}_{L1}(t) \quad \hat{i}_{L2}(t) \quad \hat{v}_c(t)\right]^T \tag{15}$$

In the vicinity of the steady state, the small signal model of the system can be obtained by the partial derivative of the variable, and the Laplace transform can be used as Eq.(16).

$$s\left[\hat{i}_{L1}(s) \quad \hat{i}_{L2}(s) \quad \hat{v}_c(s)\right]^T = A\left[\hat{i}_{L1}(s) \quad \hat{i}_{L2}(s) \quad \hat{v}_c(s)\right]^T + B\hat{v}_i(s) + \left[\frac{V_c}{L_1+L_2} \quad \frac{V_c}{L_1+L_2} \quad -\frac{I_{L1}}{C_2}\right]^T \hat{d}(s) \tag{16}$$

Make $\hat{d}(s)=0$, the transfer function of the input voltage to each state variable can be determined as Eq.(17).

$$G_{xvi} = \left(SI - A\right)^{-1} B \tag{17}$$

Make $\hat{v}_i(s)=0$, the transfer function of the duty cycle to each state variable can be calculated as Eq.(18).

$$G_{xd} = \left(SI - A\right)^{-1} \left[\frac{V_c}{L_1+L_2} \quad \frac{V_c}{L_1+L_2} \quad -\frac{I_{L1}}{C_2}\right]^T \tag{18}$$

The control structure of the AC/DC mode is shown in Fig. 5.

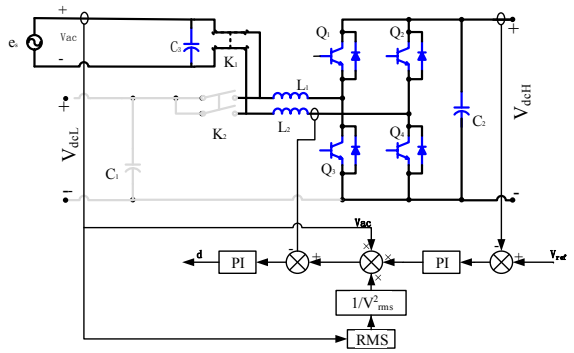

Fig. 5 The control structure of the AC/DC mode

The loop is composed of an inner current loop and a voltage outer ring. The output voltage of the PI regulator in the outer loop is multiplied by a multiplier and the input voltage, so that the output current is proportional to the input voltage. In order to keep the output power constant when the input voltage varies, the effective value of the input voltage is added as the feed forward. The signal calculated by the multiplier is used as a reference of the current loop, and the current loop is adjusted by PI regulator to obtain the control PWM signal.

2.3 DC/AC mode

The output of the DC/AC mode is sinusoidal signal, and there is no DC steady state operation point. It is a typical large signal nonlinear system, and the equivalent circuit in DC/AC mode is shown in Fig. 6.

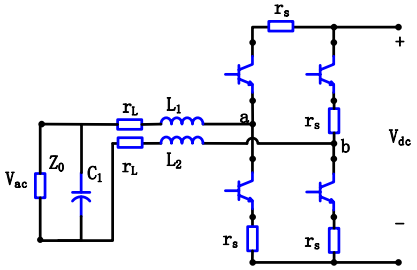

Fig. 6 The equivalent circuit in DC/AC mode

The voltage $v_c(t)$ of the capacitor C_1 and the current $i_{L1}(t)$, $i_{L2}(t)$ of inductor L_1, L_2 are selected as the state variables of the system. The voltage $v_{ab}(t)$ between the two points of 'a' and 'b' is taken as the input variable, and the output voltage $v_{ac}(t)$ is taken as the output variable. Because of $i_{L1}(t)=i_{L2}(t)$, the equation of the circuit can be expressed as Eq.(19)-Eq.(22).

$$(L_1+L_2)\frac{di_{L1}(t)}{dt}=-2r_L i_{L1}(t)-v_c(t)+v_{ab}(t) \tag{19}$$

$$(L_1+L_2)\frac{di_{L1}(t)}{dt}=-2r_L i_{L2}(t)-v_c(t)+v_{ab}(t) \tag{20}$$

$$C_2\frac{dv_c(t)}{dt}=i_{L1}(t)-\frac{v_c(t)}{Z_0} \tag{21}$$

$$v_{ac}(t)=v_c(t) \tag{22}$$

The coefficient matrix of the state space equation is shown in Eq.(23).

$$A=\begin{bmatrix} -\frac{2r_L}{L_1+L_2} & 0 & -\frac{1}{L_1+L_2} \\ 0 & -\frac{2r_L}{L_1+L_2} & -\frac{1}{L_1+L_2} \\ \frac{1}{C_2} & 0 & -\frac{1}{Z_0C_2} \end{bmatrix},\quad B=\begin{bmatrix} 1/(L_1+L_2) \\ 1/(L_1+L_2) \\ 0 \end{bmatrix},\quad C=\begin{bmatrix}0 & 0 & 1\end{bmatrix},\quad D=[0] \tag{23}$$

The voltage $v_{ab}(t)$ is a discontinuous signal, which can be averaged over a switching period to obtain its average state, and the model is solved. For unipolar modulation, when the modulation wave is $v_{ref}(t)=V_{ref}sin(\omega t)$ and the carrier amplitude is V_t, the average value of the voltage $v_{ab}(t)$ in one cycle can be expressed as Eq.(24).

$$\langle v_{ab}(t)\rangle_{Ts}=V_{dc}\frac{V_{ref}sin(\omega t)}{V_t} \tag{24}$$

Substituting Eq.(24) into the state equation of the system, the related characteristics can be solved. If the internal resistance of the two inductors is equal to r_L, the transfer function of the system can be expressed by Eq.(25).

$$G_{xvi}=(SI-A)^{-1}B \tag{25}$$

The control structure of the DC/AC mode is shown in Fig. 7.

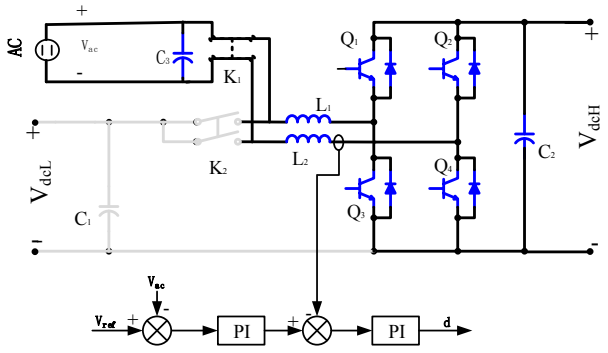

Fig. 7 The control structure of the DC/AC mode

The control system is composed of an inner loop and an outer loop. The reference signal of the voltage outer ring is the sinusoidal signal with the same output frequency. After the PI regulator, the reference signal of the current inner loop is obtained, and the PWM pulse is output after the PI regulator in the current inner loop.

3 Simulation

The inductance of L_1 and L_2 is taken as 690uH. The AC filter capacitor C_3 is set to 3 μ F. The high side filter capacitor C_2 is set to 9400 F. The low side capacitor C_1 is set to 2200 F for simulation. The Matlab/Simulink is used for simulation, the main circuit of the simulation model is shown in Fig. 8.

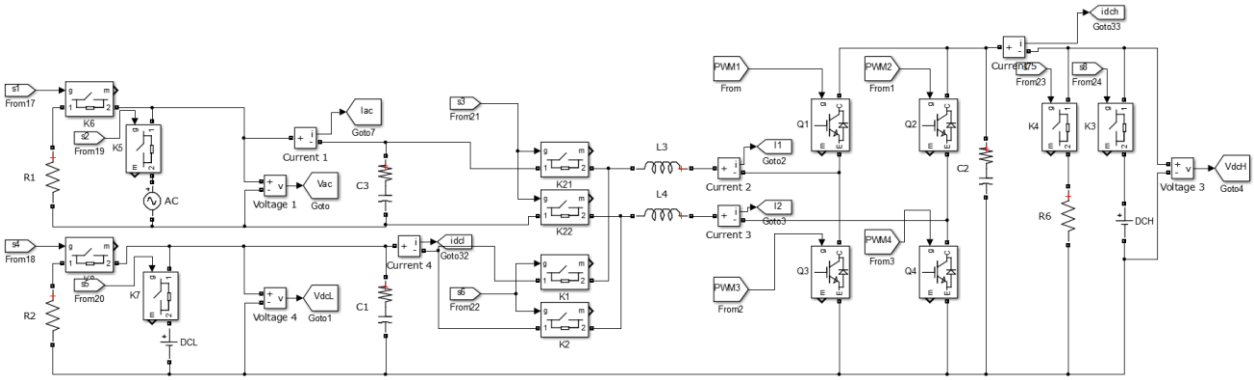

Fig. 8 Main circuit of the simulation model

3.1 Bidirectional DC/DC mode

When working in Buck mode of Bi-DC/DC mode, set the input voltage as 350V, the output voltage as 220V, the output power as 30kW, the inductor current and drive signals is shown in Fig. 9. During operation, the two IGBT turns on alternately, each phase lag 180 degrees to reduce the output current ripple.

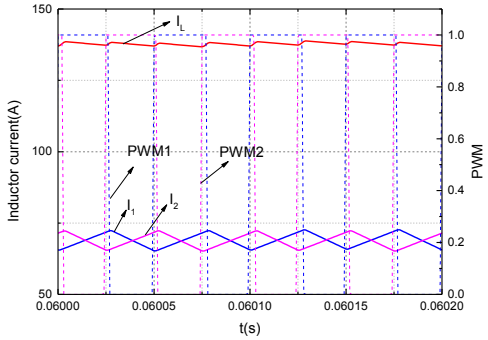

Fig. 9 Inductor current waveform in bi-directional DC/DC mode

In Boost mode, the input voltage is 220V, and the output voltage is 350V. Under the load conditions of 30kW, the output voltage response is shown in the Fig. 10(a).

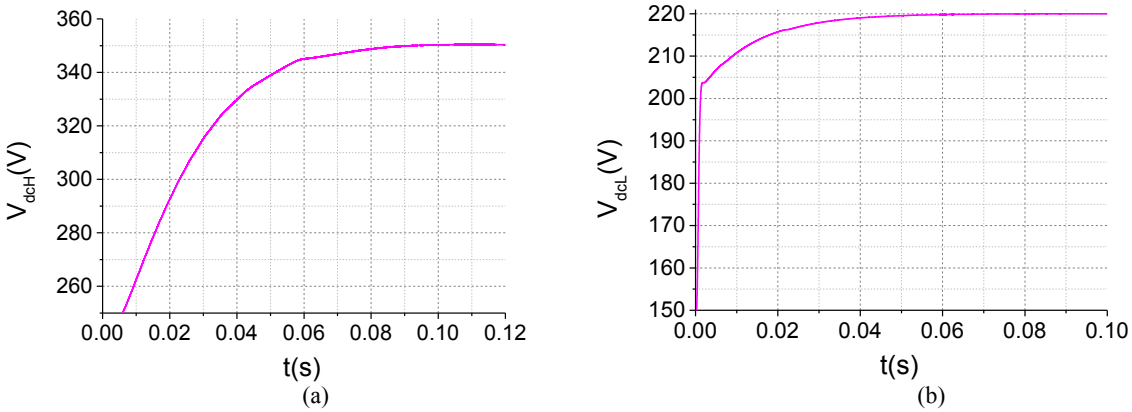

(a) (b)

Fig. 10 Output voltage waveform: (a) Boost mode; (b) Buck mode

In Buck mode, the input voltage is 350V, and the output voltage is 220V. Under different loads, the output voltage response process is as Fig. 10(b).

3.2 AC/DC mode

In AC/DC mode, as shown in Fig. 11(a), set the input voltage as 180V and 240V, simulation studies are carried out respectively. The output voltage is set to DC 400V, the load resistance is 60 ohms, and the output power is 2.667kW at steady state. The PCMM converter operates in the AC/DC mode. The single-phase AC input is rectified, and the power factor correction is completed. The input voltage and current are shown in the Fig. 11.

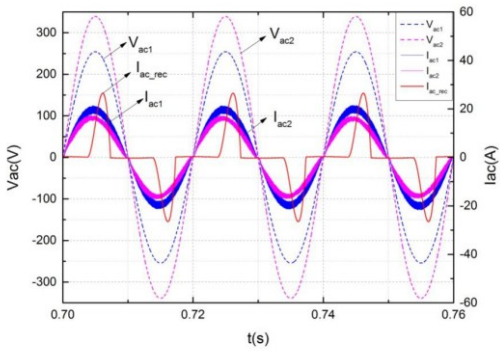

Fig. 11 output voltage and current waveform

In the Fig. 11(a), the V_{ac1} is the waveform when the input voltage RMS value is 180V, and the I_{ac1} is the corresponding input current waveform. V_{ac2} is the waveform when the input voltage RMS value is 240V, and the I_{ac2} is the corresponding input current waveform. In contrast, the I_{ac_rec} is an input current that does not use power factor correction. After the power factor correction, the input current changes proportionally with the input voltage, and the circuit presents the resistive load characteristic, and the power factor is greater than 0.996.

The input current is analysed by frequency spectrum, and each order harmonic is shown in the Tab.1. The total harmonic distortion (THD) of the input current is 6.62% for AC180V input. In the AC240V input, the THD of the input current is 8.22%, which meets the requirements of the Class A equipment in the IEC6000-3-2 standard.

Tab1 Harmonic of input current

Harmonic order	I_{h_rec}(A)	I_{h2}(A)	I_{h1}(A)	I_{hs}(A)
0	0.0000	0.0193	0.0544	
1	10.2426	15.6923	20.0396	
2	0.0000	0.0130	0.0367	1.0800
3	8.4349	0.4684	0.2735	2.3000
4	0.0000	0.0052	0.0034	0.4300
5	5.4647	0.2243	0.1358	1.1400
6	0.0000	0.0025	0.0054	0.3000
7	2.6145	0.1856	0.1163	0.7700
8	0.0000	0.0030	0.0031	0.2300
9	1.0190	0.1600	0.1143	0.4000
10	0.0000	0.0106	0.0119	0.1840
11	0.8765	0.1371	0.0942	0.3300
12	0.0000	0.0079	0.0060	0.1533
13	0.6629	0.1198	0.0861	0.2900
14	0.0000	0.0157	0.0030	0.1314
15	0.3919	0.1187	0.0911	0.2570
16	0.0000	0.0086	0.0148	0.1150
17	0.3624	0.0706	0.1022	0.2265
18	0.0000	0.0055	0.0142	0.1022
19	0.2929	0.0623	0.0682	0.2026
20	0.0000	0.0110	0.0145	0.0836

3.3 DC/AC mode

In an independent inverter mode, the output AC voltage and current phase do not need to track the phase of the grid voltage. Voltage control is used to regulate the output voltage. In inverter mode, the DC voltage is set to 400V, the output voltage RMS value is set to 220V. The output voltage and current are shown in Fig. 12.

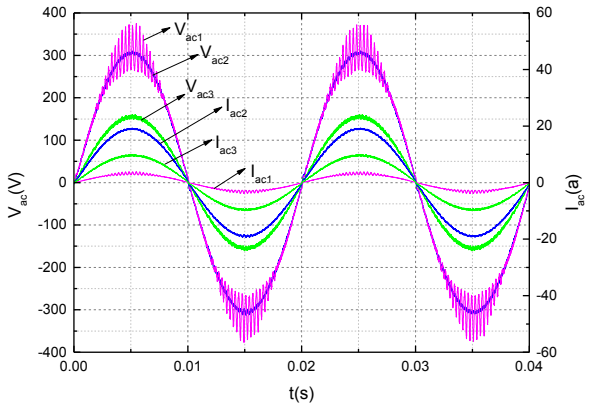

Fig. 12 output voltage and current waveform

In Fig. 12, set the RMS voltage of the output voltage is 220V, V_{ac1} , V_{ac2} and V_{ac3} is the voltage waveform when the load is 500W, 3kW and 1.5kW. I_{ac1} , I_{ac2} and I_{ac3} is the current waveform when the load is 500W, 3kW and 1.5kW.

Tab.2 Harmonic of output current

Harmonic order	I_{h1}(A)	I_{h2}(A)	I_{h3}(A)	I_{hs}(A)
0	0.0000	0.0000	0.0003	
1	3.2150	19.0148	9.6702	
2	0.0004	0.0004	0.0001	1.0800
3	0.0066	0.1150	0.0627	2.3000
4	0.0007	0.0019	0.0024	0.4300
5	0.0194	0.0660	0.0244	1.1400
6	0.0019	0.0007	0.0010	0.3000
7	0.0114	0.0398	0.0168	0.7700
8	0.0020	0.0008	0.0034	0.2300
9	0.0024	0.0317	0.0132	0.4000
10	0.0015	0.0030	0.0051	0.1840
11	0.0006	0.0355	0.0186	0.3300
12	0.0036	0.0018	0.0031	0.1533
13	0.0025	0.0268	0.0185	0.2900
14	0.0028	0.0047	0.0004	0.1314
15	0.0023	0.0326	0.0168	0.2570
16	0.0014	0.0094	0.0044	0.1150
17	0.0024	0.0233	0.0151	0.2265
18	0.0011	0.0007	0.0048	0.1022
19	0.0011	0.0247	0.0141	0.2026
20	0.0010	0.0059	0.0019	0.0836

The output current is analysed by frequency spectrum, and each order harmonic is shown in the Tab.2. The THD of the input current is 9.12%; when the load is 3kW, the output voltage value 220V, the THD of the input current is 1.53%; when the load is 1.5kW, the output voltage value 110V, the THD of the input current is 2.28%. It can meet the requirements of the Class A equipment in the IEC6000-3-2 standard.

4 Experimental

In order to reduce the inductor volume, the L_1, L_2 is 69uH/150A, in AC/DC and DC/AC modes, a series of inductor values of 1.2mH/20A are added. The filter capacitor C_3 employs a 3uF/600V capacitor, the filter capacitor C_2 employs two 4700 F/500V aluminium electrolytic capacitors, and the filter capacitor C_1 employs a 2200 F/400V aluminium electrolytic capacitor. The four switch tubes are made up of two MITSUBISHI PM200DV1A120 IPM modules. The current is sampled by a HAS-200-s LEM current sensor. The voltage sensor uses LEM's LV25-P voltage sensor to isolate the samples. The experimental test bench is shown in Fig. 13.

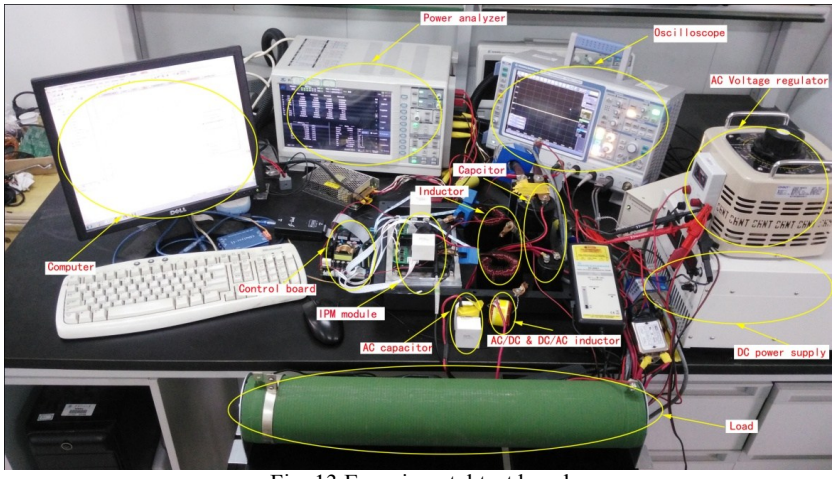

Fig. 13 Experimental test bench

4.1 Bi-DC/DC mode

The input voltage and the output voltage of the bidirectional DC/DC model are shown in Fig. 14(a) and Fig. 14(b). In the figures, the pink curves are the output voltage of the high side voltage. The blue curves are the low side voltage DC.

In Boost mode, when the input voltage is 220V, the output voltage is 350V, the load resistance is 30Ω, the input voltage and the output voltage are shown in Fig. 14(a) during the conversion start. The conversion efficiency achieves 96.4%.

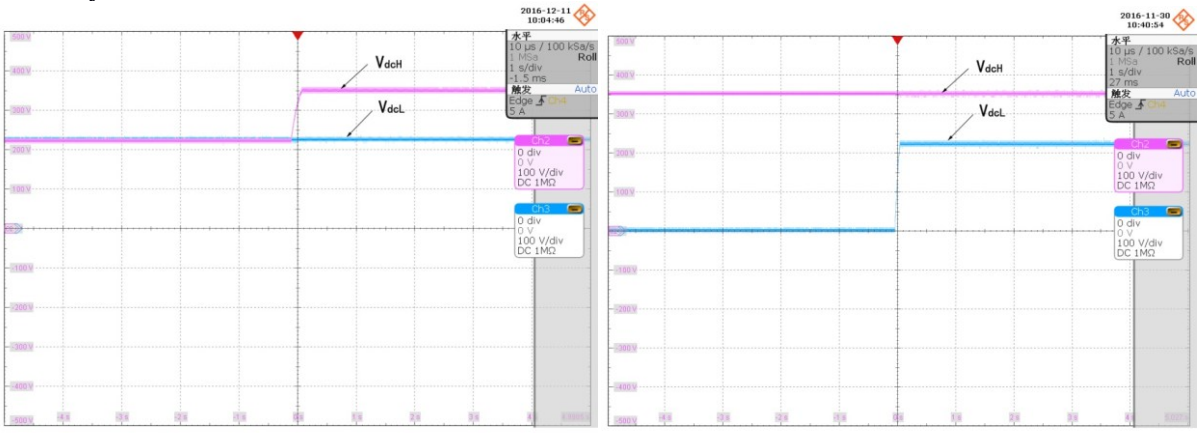

(a) (b)

Fig. 14 Input voltage and output voltage: (a) Boost mode (b) Buck mode

In Buck mode, the input voltage is 350V, the output voltage is 220V, the load resistance is 30Ω, the input voltage and output voltage are shown in Fig. 14(b) during the conversion start. The conversion efficiency is 96.1%.

4.2 AC/DC mode

The AC voltage end adopts 3kVA transformer to adjust the grid voltage as input. DC terminal connection resistance load. When the PFC circuit is not started, the four reverse diode form a bridge rectifier, and the

circuit operates in the uncontrolled rectifier state. The input voltage and current at the AC terminal are shown in Fig. 15(a). The power factor is 0.57, and the output voltage is uncontrollable.

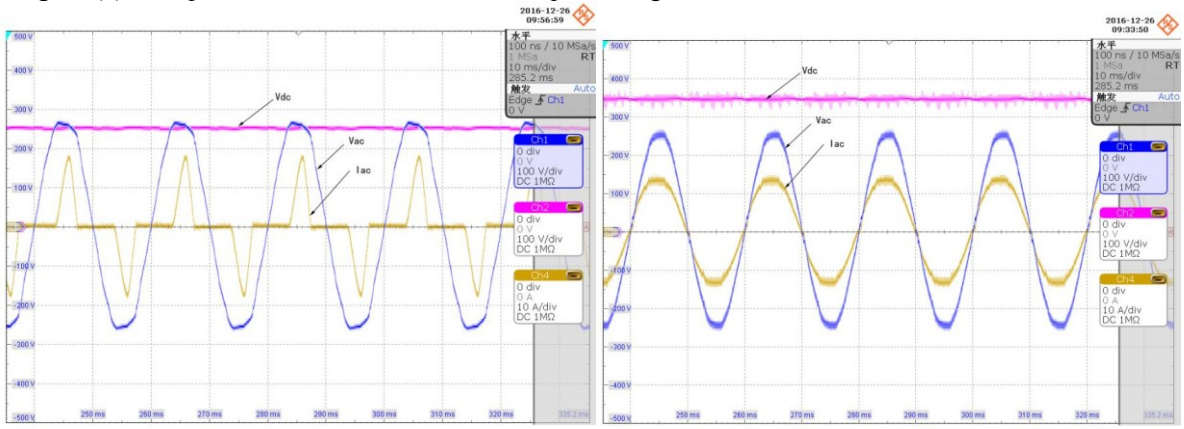

Fig. 15 Voltage and Current in AC/DC mode: (a) without power factor correction; (b) with power factor correction

After adopting the bridgeless PFC, the output voltage is set as DC 350V, and the input current is proportional to the input voltage. The input voltage, the input current and the output DC voltage are shown in Fig. 15(b). After power factor correction, the power factor is increased to 0.988. The conversion efficiency is 96.4%, the I_{thd} is 5.68%, and the output voltage is stable under the regulation of the regulator.

4.3 DC/AC mode

In the inverter mode, as shown in Fig. 16(a), the input voltage is DC350V, the output voltage effective value is AC 220V, the load resistance is 54, the frequency is 50Hz. The pink curve is the DC high voltage terminal, the blue curve is the output voltage of the inverter mode, and the Yellow curve is the output current of the inverter mode. The output current of THD is 5.893%, the efficiency is 96.7%.

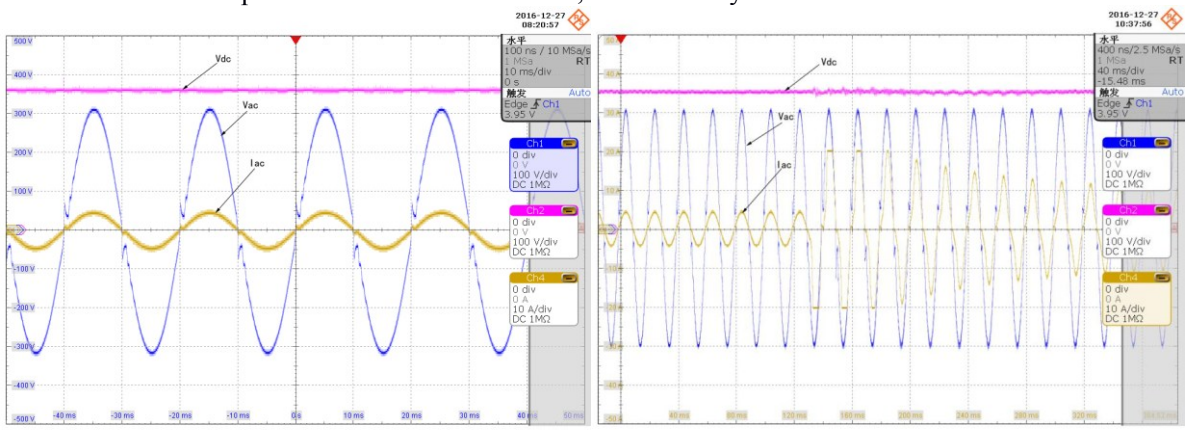

(a) (b)

Fig. 16 (a) Output voltage, output current and output voltage of DC/AC
(b)Waveform with motor load

In order to verify the performance of the inverter with motor load, the 900W AC motor is used as the load. Waveform as shown in Fig. 16(b), in the load change process, the AC side output power is 1800W, the conversion efficiency is 96.7%.

5 Conclusions

The proposed integrated multifunctional power conversion system can work in Bi-DC/DC, AC/DC, DC/AC mode. A typical application is the super-capacitor + battery hybrid energy storage system. Bi-DC/DC mode converts the power between the battery and the super-capacitor; AC/DC mode can charge the battery; DC/AC mode can provide AC source to electrical equipment, and can also return energy to the grid. Analysis of the technology specific design trends concludes:

(1)In Bi-DC/DC mode, the conversion efficiency achieves 96.4% in Boost mode and 96.1% in Buck mode.

(2)In AC/DC mode, the power factor is increased to 0.988, the conversion efficiency is 96.4%. The I_{thd} is 5.68%, which meets the requirements of the Class A equipment in IEC6000-3-2 standard.
(3)In DC/AC mode, the efficiency is 96.7%, the output current of THD is 5.893%, which meets the requirements of the Class A equipment in IEC6000-3-2 standard.

Acknowledgments

The authors gratefully acknowledge the Major Research and Development Project of Guangdong Provincial Department of Science and Technology. The research work was undertaken in the “The Research of the Constant Temperature Control and Long Life HESS for the Electric Vehicle”, (2016B010132001).

References

[1] H. Wen and B. Su, "Hybrid-mode interleaved boost converter design for fuel cell electric vehicles," *Energy Conversion & Management,* vol. 122, pp. 477-487, 2016.
[2] H. Xu, X. Wen, E. Qiao, and X. Guo, "High Power Interleaved Boost Converter in Fuel Cell Hybrid Electric Vehicle," in *IEEE International Conference on Electric Machines and Drives*, 2005, pp. 1814-1819.
[3] D. P. Urciuoli and C. W. Tipton, "Development of a 90 kW bi-directional DC-DC converter for power dense applications," in *IEEE*, 2006, p. 4 pp.
[4] S. J. Jang, C. Y. Won, B. K. Lee, and H. Jin, "Fuel Cell Generation System With a New Active Clamping Current-Fed Half-Bridge Converter," *IEEE Transactions on Energy Conversion,* vol. 22, pp. 332-340, 2007.
[5] B. Su, J. Zhang, and Z. Lu, "Totem-Pole Boost Bridgeless PFC Rectifier With Simple Zero-Current Detection and Full-Range ZVS Operating at the Boundary of DCM/CCM," *IEEE Transactions on Power Electronics,* vol. 26, pp. 427-435, 2011.
[6] K. S. Muhammad and D. C. Lu, "Two-switch ZCS totem-pole bridgeless PFC boost rectifier," in *IEEE International Conference on Power and Energy*, 2012, pp. 1-6.
[7] J. Y. Lee, H. S. Song, I. P. Yoo, K. Y. Jang, S. Shin, and J. H. Joo, "System for recharging plug-in hybrid vehicle and control method for the same," ed: US, 2013.
[8] S. Dusmez, C. Chen, and A. Khaligh, "A reduced-part single stage direct AC/DC On-board charger for automotive applications," pp. 1791-1797, 2013.
[9] S. Dusmez and A. Khaligh, "A Charge-Nonlinear-Carrier-Controlled Reduced-Part Single-Stage Integrated Power Electronics Interface for Automotive Applications," *IEEE Transactions on Vehicular Technology,* vol. 63, pp. 1091-1103, 2014.

Authors

Luo Yutao was born in Shandong, China, in 1972. He received the B.Sc., M.Sc., and Ph.D. degrees from South China University of Technology, Guangzhou, China, in 1993, 1996, and 2002,respectively.He is a Professor of Department of Automotive Engineering, School of Mechanical and Automotive Engineering, South China University of Technology. His research interests are the energy storage systems, the motor design, and control of electric vehicles.

Wang Feng was born in Yunnan, China, in 1983. He received the B.Sc. in 2005 from Southeast University, Nanjing, China, and M.Sc. degrees in 2011 from Southwest Forestry University, Kunming, China. He is currently working toward the Ph.D. degree in South China University of Technology, Guangzhou, China. His research interests include energy storage system of electric vehicles.